

Highly clustered mating networks in naturally fragmented riparian tree populations

Eva Moracho¹ | Etienne K. Klein^{2,3}  | Sylvie Oddou-Muratorio² | Arndt Hampe^{4,5} | Pedro Jordano^{1,6} 

¹Integrative Ecology Group, Estación Biológica de Doñana (EBD-CSIC), Sevilla, Spain

²Ecologie des Forêts Méditerranéennes, UR 629, INRA, Avignon, France

³Biostatistique et Processus Spatiaux, UR 546, INRA, Avignon, France

⁴INRA, UMR1202 BIOGECO, Cestas, France

⁵Univ. Bordeaux, UMR1202 BIOGECO, Talence, France

⁶Dept. Biología Vegetal y Ecología, Universidad de Sevilla, Sevilla, Spain

Correspondence

Pedro Jordano, Integrative Ecology Group, Estación Biológica de Doñana (EBD-CSIC), Av. Américo Vespucio 26, Isla de la Cartuja, E-41092 Sevilla, Spain.
Email: jordano@ebd.csic.es

Funding information

Spanish Ministry of Science, Innovation, and Universities, Grant/Award Number: PID2022-136812NB-I00 and CGL2010-18381; LifeWatch ERIC-SUMHAL, Grant/Award Number: LIFEWATCH-2019-09-CSIC-13; FEDER-EU funding; Universidad de Sevilla, Grant/Award Number: 2021/00000826

Handling Editor: Loren Rieseberg

Abstract

Understanding how spatial patterns of mating and gene flow respond to habitat loss and geographical isolation is a crucial aspect of forest fragmentation genetics. Naturally fragmented riparian tree populations exhibit unique characteristics that significantly influence these patterns. In this study, we investigate mating patterns, pollen-mediated gene flow, and genetic diversity in relict populations of *Frangula alnus* in southern Spain by testing specific hypotheses related to the riparian habitat. We employ a novel approach that combines paternity analysis, particularly suited for small and isolated populations, with complex network theory and Bayesian models to predict mating likelihood among tree pairs. Our findings reveal a prevalence of short-distance pollination, resulting in spatially driven local mating clusters with a distinct subset of trees being highly connected in the mating network. Additionally, we observe numerous pollination events over distances of hundreds of metres and considerable pollen immigration. Local neighbourhood density is the primary factor influencing within-population mating patterns and pollen dispersal; moreover, mating network properties reflect the population's size and spatial configuration. Conversely, among-population pollen dispersal is mainly determined by tree size, which influences floral display. Our results do not support a major role of directional pollen dispersal in longitudinal trends of genetic diversity. We provide evidence that long-term fragmented tree populations persist in unique environments that shape mating patterns and impose constraints to pollen-mediated gene flow. Nevertheless, even seemingly strongly isolated populations can maintain functional connectivity over extended periods, especially when animal-mediated mating networks promote genetic diversity, as in this riparian tree species.

KEYWORDS

Bayesian mating models, climate refugium, long-distance dispersal, mating network, paternity analysis, plant–animal interactions, pollination, relict

1 | INTRODUCTION

Riparian ecosystems around the world are disproportionately threatened by landscape transformation and the fragmentation of natural habitats (Dudgeon et al., 2006; Grill et al., 2019; Lindenmayer & Fischer, 2013). In conservation biology, assessing the effects of habitat fragmentation on the genetic structure, fitness, and viability of populations persisting in remnant habitat patches is a central goal (Young & Clarke, 2000). Many studies have documented that fragmented plant populations tend to show reduced allelic richness, genetic diversity, heterozygosity, and individual fitness (Aguilar et al., 2008, 2019). One way to mitigate the negative effects of fragmentation on riparian plant species is to preserve habitat connectivity (Haddad et al., 2015). However, ensuring that different habitat patches are effectively connected requires a precise understanding of how genes and individuals disperse (Baguette et al., 2013). Documenting contemporary levels and patterns of within- and among-population gene flow in riparian plant populations can thus help to generate predictions about their current isolation and to diagnose potential early stages of decline.

Riparian habitats share unique features that have significant implications for the connectivity, genetic structure, and diversity both within- and among-populations (Blanchet et al., 2020). First, the dendritic structure of rivers tends to limit the number of nearby mates and access to more distant ones. This results in a predominance of short-distance mating, reduced pollen donor diversity, an increased fraction of full-sibs in the offspring, and, ultimately, the formation of highly structured pedigrees and the reduction of genetic diversity. The phenomenon is of minor importance in wide gallery forests growing along large lowland rivers (Bertolasi et al., 2015; Cushman et al., 2014; Goto et al., 2006), but can be far more relevant in smaller rivers that sustain only narrow fringes of riparian vegetation (Hoshikawa et al., 2012; Manoel et al., 2017; Ouayjan & Hampe, 2018). In such conditions, immigration from other catchments can be critical to maintaining diversity in the long term (Moracho et al., 2016; Werth & Scheidegger, 2014). In these scenarios, the loss of local population nodes may severely impair connectivity (Sarker et al., 2019). Second, many riparian plant species disperse their propagules (seeds or vegetative units) by water flow, creating unidirectional, longitudinal trends in the genetic structure of populations. Downstream increases of diversity or decreases of small-scale pedigree structures (a phenomenon described by the 'unidirectional diversity hypothesis'; see Blanchet et al., 2020, for a detailed review) are common in waterborne taxa, but the empirical support for plants is weak (Honnay et al., 2010; Paz-Viñas et al., 2015). A common, albeit rarely tested, explanation for this absence of a general trend is that overland pollen transfer (e.g. by insects or air currents) could blur the otherwise expected downstream increase in genetic diversity. Overall, pollen flow in riparian plant populations is hence constrained by their spatial configuration and is particularly relevant for the long-term preservation of their genetic diversity.

Understanding pollen-mediated gene flow patterns requires individual-based approaches where mating events among individual

trees, and their consequences, can be recorded. The mating events occurring in each reproductive episode link individual pairs as reproductive partners so that a mating network describes the form (topology) and structure of how these matings occur (Rodríguez-Rodríguez et al., 2017). Complex network theory (Barabási & Pósfai, 2016) provides metrics to characterize the 'positions' of individual trees within these mating networks, for example how 'central' an individual is both in terms of exchanging (donating or receiving) pollen with other individuals in the population and in terms of receiving pollen from other populations. Riparian tree populations may have mating networks that differ markedly from more continuous, extensive stands, potentially leading to situations of pollination limitation or extremely assortative mating. Whether their particular context confers a distinct signal in mating patterns remains largely unexplored due to limitations for a proper assessment of the full range of mating events performed by individual trees and the lack of a robust theory of genetic networks at both intra- and inter-population scales (Dyer, 2015). Tools of complex network theory applied to mating networks allow us to characterize the full mating pattern of populations, and to identify distinct subsets of trees within assortative mating clusters, or individual trees that act as actual 'bridges' connecting tree clusters that would otherwise exhibit pollen flow collapse (see Dyer, 2015, Rodríguez-Rodríguez et al., 2017). Individual trees with such central mating positions can be effectively identified and are key to ensuring effective mating success in these riparian populations.

Genetic effects of fragmentation in tree populations have been found to be less evident compared to other plant life forms (Bacles & Jump, 2011; Kramer et al., 2008). This lack of signal could be due to the relative short time since the onset of the fragmentation, making it difficult to detect genetic signals in these long-lived organisms, or to life history characteristics that make trees generally resilient to the loss of genetic diversity as the capacity for long dispersal distances (Kremer et al., 2012; Petit & Hampe, 2006). It is not yet clear whether current evidence simply reflects a lagged response of tree populations to fragmentation (implying that effects will considerably increase in the future) or a greater tolerance to fragmentation (implying that effects will not significantly increase). Fragmented tree populations can be found in many landscapes, including stands that have naturally been fragmented over extended periods of time (Bacles & Jump, 2011) and can therefore provide insights into how small and isolated tree populations maintain their genetic diversity and functionality in the long term. Despite this, few studies have to date focused on such long-term fragmented 'relict' populations to address mating and pollen dispersal patterns, particularly in riparian contexts (but see Ahmed et al., 2009; Moracho et al., 2016; Ouayjan & Hampe, 2018). Thus, we have a limited understanding of the evolution of such populations to forecast their reaction to environmental changes, such as the balance between short- and long-distance gene dispersal or the level of heterogeneity in male and female fecundity (Tonnabel et al., 2021).

In this study, we investigate effective pollen movement and population-scale mating patterns in naturally fragmented small

populations of *Frangula alnus* Mill. (Rhamnaceae), an insect-pollinated, hermaphroditic tree species that grows in isolated climate microrefugia near the southern limit of its range. These populations are restricted to narrow riparian forests in ravines cut into steep coastal mountain chains. These populations provide an excellent model for investigating mating patterns in naturally fragmented riparian tree populations due to their outstanding geographical and ecological stability. The riparian forests in which these populations grow have putatively remained largely unchanged in extent or distribution for thousands of years and have been very little affected by human activities over the past decades. Ecological field studies have shown that these *F. alnus* populations experience notable pollen limitation, tree size effects on seed set, and strong individual inequality in female fecundity, as well as considerable downstream secondary seed dispersal by winter peak water flows on top of zoochorous seed dispersal (Hampe, 2004, 2005).

We conducted paternity analysis of known *F. alnus* progenies and modelling of causal factors of heterogeneity in mating patterns in four populations of different size, density, neighbourhood structure, and isolation. We also predicted mating networks for each population using a Bayesian mating model that infers individual male fecundity and the pollen dispersal kernel. Specifically, our study addresses four hypotheses: (H1) Within-population pollen dispersal is driven by the spatial distribution of mates, with a predominance of short-distance pollination, reduced numbers of effective fathers, and high kinship of the progenies. (H2) Populations exhibit highly structured mating networks, reflecting the strong spatial clustering and directionality imposed by the riparian habitats, with small, distinct subsets of trees playing a central role in mating and pollen-mediated gene flow. (H3) Pollen immigration occurs at very low rates and preferably at the topographically most accessible population extremes, such as headwaters or downstream limits. (H4) Populations show a downstream increase in genetic diversity linked to waterborne dispersal of propagules.

2 | MATERIALS AND METHODS

2.1 | Study species

Frangula alnus Mill. (Rhamnaceae) is a deciduous shrub or tree distributed through much of Europe (Meusel et al., 1978). The subspecies *F. alnus* subsp. *baetica* (Rev. and Willk.) Rivas Goday ex Devesa occurs sparsely across mountain ranges of southern Spain, where populations have probably been continuously present since the Neogene (Hampe et al., 2003). These populations are restricted to the understory of 10–20 m wide riparian forests that extend from about 100 m to a few kilometres along streams and are surrounded by extensive Mediterranean sclerophyllous and semideciduous forests (Hampe & Arroyo, 2002). Despite their small extension, these riparian forests have apparently been outstandingly persistent through time and serve today as a 'climate refugium hotspot' for numerous woody and fern species of Neogene origin (Rodríguez-Sánchez et al., 2008). On

the other hand, the local topography has historically set strict and invariable spatial limits to their spatial distribution, with the upper bound being defined by the headwaters and the lower bound by the opening of the gorges and associated steep changes in edaphology, water flow, and microclimate. The target populations are located in the 'Los Alconocales' Natural Park and have been under strict protection since its establishment in 1987. Outside this area, *F. alnus* subsp. *baetica* is in accelerated decline and is included in the Spanish National Red List as vulnerable according to IUCN standards.

The reproductive biology of *F. a. baetica* has been described in detail by Medan (1994) and Hampe (2005). This self-incompatible species depends on sexual reproduction for regeneration as it can readily resprout but does not reproduce vegetatively. Its small hermaphroditic, protandrous flowers are produced from mid-April to mid-June and are pollinated by a wide array of insects with predominance of Hymenoptera and Diptera. Field experiments have revealed a marked pollen limitation and an effect of flower visibility on pollination success (Hampe, 2005). Seed set is greater in trees with a large flower display, probably because they are more likely to intercept insect pollinators arriving from greater distances. Fruits are black berries with two or three one-seeded stones that ripen between late June and early September and are eaten and dispersed by birds (Hampe & Arroyo, 2002). In addition, extensive downstream seed dispersal over hundreds of metres occurs regularly during peak water flows following winter rains (Hampe, 2004). Importantly, this water dispersal tends to deposit seeds in suitable microhabitats for plant establishment whereas many bird-dispersed seeds end up outside the riverbed and are thus lost for regeneration (Hampe, 2004). Hampe and Arroyo (2002) reported highly skewed fruit crop size distributions and a clear correlation of fruit crop size with tree age and height, concluding that the effective size of *F. alnus* subsp. *baetica* populations is probably even much smaller than the already limited number of individuals recorded in the field.

2.2 | Sampling design

Field work was carried out between April and August 2009 in four natural *F. alnus* populations located in the Sierra del Aljibe mountain range (Cádiz province, southern Spain; see Table 1): Juan Vela (JV), La Saucedá (SAUC), Pasada Llana (PLLA), and El Zapato (ZAPA). These populations exhibit a linear spatial structure, with dense vegetation along the streams. Within each population, we carefully searched, GIS-mapped and tagged all *F. alnus* trees with a stem diameter at breast height (dbh) >5 cm (see Figure S1). This threshold was chosen following the observation that trees usually start to produce fruits when they have attained a dbh around 6 cm (Hampe & Arroyo, 2002). We collected leaf material of each tree ($n=498$) for DNA analyses. During the fruiting season, we selected 7 to 12 trees within each population and collected around 50 fruits from each tree (Figure S1). The selected trees were distributed throughout the population area and captured the structural heterogeneity of the ravines. Between 15 and 30 of the fruits were then randomly chosen, and a single seed was extracted from each fruit for analyses (mean = 22 seeds/tree).

	JVEL	SAUC	PLLA	ZAPA
Geographic coordinates	36°30'42" N 5°38'27" W	36°32'11" N 5°36'16" W	36°31'17" N 5°35'25" W	36°28'44" N 5°37'19" W
No. trees	40	88	144	226
Stream length (m)	290	520	2200	1500
Area (m ²)	3725	10,400	92,000	45,000
No. seeds genotyped	205	117	176	162
A_o	60 ^a	73 ^a	86 ^a	90 ^a
A_p	0.00 ^a	0.56 ^{ab}	0.75 ^b	0.94 ^b
H_o	0.40 ^a	0.49 ^a	0.49 ^a	0.47 ^a
H_e	0.39 ^a	0.50 ^a	0.51 ^a	0.47 ^a
F_{IS}	0.024 ^{ns}	0.015 ^{ns}	0.044 ^{ns}	0.027 ^{ns}
β_{WT} (CI)	0.27 (0.20– 0.37) ^a	0.07 (0.02– 0.11) ^b	0.05 (0.01– 0.09) ^b	0.10 (–0.02 to 0.25) ^{ab}
PEP	0.982	0.997	0.998	0.997
Assigned (%)	63.4	91.5	92.2	79.0
Selfing (%)	4.9	2.6	3.0	0.6
Unassigned (%)	30.7	0	0	16.0
Immigration (%)	5.9	8.5	7.8	4.9
Median/mean dispersal distance (m)	22/38	26/54	104/188	26/189

Note: Paternity assignments with CERVUS can produce, for each individual seed, either a uniquely identified pollen donor (which can be the mother tree itself, indicated as selfing), an unresolved paternity with more than one possible pollen donor (indicated as unassigned), or all trees in the population being excluded as potential pollen donors (indicated as immigration). A_o : number of alleles observed; A_p : mean number of private alleles per locus; H_o and H_e : observed and expected heterozygosity; F_{IS} : inbreeding coefficient (computed with FSTAT v. 2.9.3; Goudet, 1995); β_{WT} : population-specific index of genetic differentiation (function *betas* in package 'hierfstat'; Weir & Goudet, 2017; R v.4.2.0, R Development Core Team, 2022); PEP: paternity exclusion probability (estimated with CERVUS; Marshall et al., 1998). F_{IS} departures from zero were tested using 5000 permutations: ^{ns} $p > .05$. Superscripts with the same letter indicate non-significant differences among populations ($p < .05$) according to one-way ANOVAs followed by Tukey tests.

Our decision on this sample size was based on a previous analysis of genetic diversity accumulation curves of sampled progenies (using 30 seeds per tree) in 10 mother trees in population JVEL (Figure S2). The analysis (function *specaccum* in package 'vegan'; Oksanen et al., 2013; R v.4.2.0, R Development Core Team, 2022) estimated the asymptotic genetic diversity of each progeny and indicated that 15 seeds per mother adequately describe the genetic diversity of seed families (see Figure S2). The final sample included a total of 772 genotyped seeds originating from 35 mother trees.

2.3 | Microsatellite genotyping and quality of the marker set

Sampled leaves were dried and stored in silica gel, while fruits were frozen and stored at –20°C until DNA isolation. Seeds were separated from the pulp, and the embryo was carefully extracted from the seed endocarp and seed coat. Nuclear DNA was isolated from leaves and seeds using a standard cetyltrimethyl ammonium bromide

(CTAB) extraction method (Milligan, 1998) with minor modifications (Rigueiro et al., 2009). All samples were scored at 16 microsatellite markers: FaA103, FaA12, FaB102, FaB101, FaA110, FaB7, FaA104, FaB106, FaB4, FaA125, FaA7, FaA116, FaA3, FaA8, FaB8, and FaB9 (FJ375935–FJ375950 – GenBank ID), following the procedure described in Rigueiro et al. (2009). One reference sample and a negative control were included in all amplifications to check for contamination and to standardize the size of allele fragments across plates. Amplified fragments were analysed using an ABI 310 Capillary Electrophoresis system (Applied Biosystem), and fragment sizes were assessed using GeneMapper version 4.0 (Applied Biosystem). Allele scoring was independently performed by two persons, and so scores were double-checked manually in order to minimize scoring errors. We also quantified the genotyping error rate using 48 randomly chosen seeds as blind samples. Three independent extractions, amplifications, and analyses of each blind sample, respectively, resulted in an estimated overall genotyping error rate of 0.98% ($n = 768$ scorings). Testing for linkage disequilibrium in FSTAT v. 2.9.3 (Goudet, 1995) revealed no significant linkage between loci. Null allele frequencies per

TABLE 1 Population features, adult genetic diversity, mating system parameters, and pollen dispersal distances for each of the four *Frangula alnus* subsp. *baetica* populations (JVEL, Juan Vela; SAUC, La Saucedá; PLLA, Pasada Llana, and ZAPA, El Zapato).

locus and per population were estimated using the software ML-null (Kalinowski et al., 2006). All but one locus (FaA3) in JVLE and another locus (FaA116) in PLLA showed frequencies below 0.05. The genotypes of all analysed trees differed in at least one allele (usually more). The paternity exclusion probability (i.e. the likelihood to exclude a randomly chosen nonfather based on allele frequencies) was estimated in CERVUS version 3.0 (Kalinowski et al., 2007).

2.4 | Spatial genetic structure (SGS)

Spatial autocorrelation of kinship coefficients was investigated for the adult trees of the four populations. Kinship coefficients (F_{ij}) were computed for all pairs of individuals within each population using the statistic of Loiselle et al. (1995), as implemented in SPAGeDi version 1.2 (Hardy & Vekemans, 2002). Confidence intervals around each F_{ij} value were obtained through a jackknife procedure over loci. To test SGS, the kinship values were regressed on $\ln(d_{ij})$, where d_{ij} is the spatial distance between individuals i and j , and the significance of the regression slope ($b_{\log F}$) was assessed using 5000 permutations of genotypes among individual's positions within each population.

2.5 | Categorical paternity analysis

The paternity of each offspring was determined by maximum-likelihood methods with CERVUS 3.0 (Kalinowski et al., 2007), assuming the strict confidence criterion (95%). No mother-progeny mismatches were found in the whole sample of genotyped seeds ($n=772$), suggesting a high quality of the genotyping. Considering our empirical estimate of genotyping error (see above), we set an error rate of 1%. For each population, we ran 50,000 simulations with the same sample size and allele frequency as the focal population to estimate the statistical confidence threshold for assignment. We considered a complete sampling of potential candidate fathers since very low levels of pollen immigration can reasonably be assumed given our high-isolation context (Moracho et al., 2016; Ouayjan & Hampe, 2018) and since this is also the most conservative strategy when considering error rates (Oddou-Muratorio et al., 2003). Following the paternity assignment, we built a frequency distribution of inter-mate distances based on progenies that were assigned to a unique candidate father within each population (including selfing). Otherwise, seeds were attributed either to immigration (when all trees were excluded as potential fathers) or unassigned paternity (when more than one candidate father could be the true father).

2.6 | Ecological correlates of progeny genetic diversity

We attempted to identify the ecological determinants of the genetic diversity of the pollen clouds received by the mother

trees sampled in each population. The following response variables were calculated for each progeny: unbiased gene diversity (H_E) and inbreeding coefficient (F_{IS}), obtained with FSTAT v. 2.9.3 (Goudet, 1995); mean kinship of progeny, computed for all possible pairs of seeds from each mother using the kinship coefficient of Loiselle et al. (1995), as implemented in SPAGeDi 1.3 (Hardy & Vekemans, 2002); median dispersal distance, effective number of pollen donors (N_{ep}) and percentage of immigration as derived from the CERVUS output (see above). Pairwise spatial distances among mates were calculated using a Euclidean distance function in R v.4.2.0 (R Development Core Team, 2022). We considered three predictor variables that define the mating environment at several scales: (i) the diameter at breast height (dbh) of the focal tree (as a proxy for tree size), (ii) the number of conspecific trees within a radius of 15 m (as a measure of the fine-scale spatial population structure and mating environment), and (iii) the sector of the ravine where the focal tree is located (as a measure of the meso-scale population structure and mating environment).

We fitted General Linear Mixed Models (GLMMs) in a maximum likelihood, multi-model inference framework in R v.4.2.0 (Anderson & Burnham, 2002; R Development Core Team, 2022) with dbh, neighbourhood density and sector of the ravine as fixed effects and the population as random effect for each response variable (H_E , F_{IS} , mean kinship of progeny, median dispersal distance, N_{ep} , and percentage of immigration). The median dispersal distance was log-transformed, under the assumption that pollen dispersal exhibits an exponential decay with increasing distance from the source (Paradis et al., 2002). We specified binomial errors to fit models for the number of pollen donors and the percentage of immigration using a *glmer* function (package 'lme4'), while the remaining variables (following a gaussian distribution) were fitted by a *lme* function (package 'nlme'). We built, for each response variable, a full model including all predictor variables and some biological relevant interactions among them. We then performed a stepwise variable selection procedure through AICc minimization criteria (Anderson & Burnham, 2002) using the package 'AICcmodavg' (Mazerolle, 2020). Goodness-of-fit was determined only on the model with the lowest AICc, calculating marginal and conditional R^2 values following Nakagawa and Schielzeth (2013) and using the *rsquaredGLMM* function in the 'MuMIn' package.

2.7 | Spatially explicit mating model

We used a Bayesian model implemented in the program Mixed Effect Mating Model (MEMM; Klein et al., 2008) to jointly estimate individual male fecundities and a pollen dispersal kernel for each population. This approach uses the genotypic information from sampled seeds and their putative fathers as well as the spatial location of all individuals in the population. Here, we used the model for generating a mating network describing the likelihood of pollen movement between each pair of individuals in the population, while accounting for immigrant pollen. Hence, we considered

that each seed, i , collected on a mother tree, j , can be sired (i) by a tree located outside the population (immigration), with a probability of m ; (ii) by the mother tree (selfing) with a probability of s ; or (iii) by another tree within the study site with a probability of $1-m-s$. For modelling the pollen dispersal kernel, that is, the proportion of pollen released at the source point $(0, 0)$ that contributes to the pollen pool at point (x, y) , we used the exponential power family. The mean dispersal distance (δ) and shape parameter (b) summarized the dispersal function of each population. We modelled the relative male individual fecundities as random variables that follow a log-normal distribution of mean 1 and variance Σ^2 , and derived the ratio between observed and effective male density ($d_{\text{obs}}/d_{\text{ep}}$) (Klein et al., 2008). We accounted for two types of mistyping at microsatellite loci: in the first type, the allele read differs only by one motif repeat from the true allele with a probability p_{err1} (here, .005), while in the second type, the allele read can be any allele observed at this locus with a probability p_{err2} (here, .005). The initial, minimum, and maximum values considered for the Markov chain in this Bayesian approach were respectively 100, 0, and 10,000 for δ ; 1, 0.01, and 10 for b ; 0.05, 0.1, and 1 for m ; 2, 1, and 1000 for $d_{\text{obs}}/d_{\text{ep}}$; and 0.5, 0 and 1 for s . For each population, we ran five MCMC chains, each of 50,000 steps, eliminated the 500 first MCMC steps as burn-in, checked that the different chains converged to the same value visually, and then combined the 5 chains together (247,500 iterations).

2.8 | Individual-based mating networks

The inferred patterns of mating events derived from MEMM allow assessing the mating structure of the studied populations. MEMM yields estimates of the frequency of mating events expected among pairs of individual trees so that the whole structure and complexity of the mating patterns can be explored. We constructed a weighted, individual-based, unipartite-directed network between all individual trees for each of the four populations. To do so, we inferred a global pollination matrix using the estimated dispersal kernel (median b and δ across the 247,500 iterations) and relative individual fecundities, together with the location of all trees within each population. This results in a symmetric matrix of pollen transfer probability, where the row vectors represent trees acting as potential fathers, and the column vectors represent trees acting as potential mothers (note that each plant of the population has one row and one column). Within a given column (mother), each cell estimates the relative fraction of pollen in its pollen cloud coming from each father, with the total summing to one. We employed a spatially explicit approach to generate visual representations of the mating network over the population maps, with the predicted matrix obtained from MEMM serving as the adjacency matrix that describes the network (Albert & Barabási, 2002). To improve the visualization of the mating network (especially for larger populations) we applied a threshold MEMM probability value of $>.05$ to define mating events in the predicted matrix, below which we

consider that no link between pairs of trees exists (i.e. mating events extremely unlikely). This threshold value was used solely for visualization purposes, and we acknowledge that very low mating likelihoods may be recorded and reflect biologically relevant events under some circumstances (e.g. long-distance pollination, successful fruit set in very isolated individuals).

To assess among-population variation in mating network topologies, a set of network metrics was computed for each population. To detect densely connected groups of nodes (e.g. trees that tend to interact with the same subset of individual trees), with sparse connections to nodes in other groups, we calculated modularity (Olesen et al., 2007). Weighted connectance (wC) is a metric that reflects the number of links in a network relative to the maximum possible number of links (Bersier et al., 2002), in our case indicating how densely connected a given mating network is. To evaluate the hierarchical structure of the mating networks, we used nestedness (NODF). High NODF values indicate the presence of a tightly knit core of highly connected nodes (trees), coupled with increased connectance of peripheral nodes, that contributes to the overall cohesion of the network (Bascompte et al., 2003). Linkage density is the mean number of links per individual that represents the amount of mating links added to the network for every additional individual tree in the population. The Shannon diversity index was used to estimate the overall diversity of the mating patterns among trees (i.e. how diversified are the combinations of pairs of trees in the mating network). A mating network with high Shannon diversity implies a more ample spread of mating events among individuals when compared to other stands with lower values of this metric, where most mating events might be dominated by a few, distinct trees. All these metrics were computed with the R package 'bipartite'. We subsequently compared network metrics among populations by estimating bootstrapped confidence intervals for each metric based on random sampling of the b and δ posterior distributions of parameters ($n=100$ randomizations). Finally, we estimated the assortativity degree of the mating networks for each population (Newman, 2002). Assortativity is expected when matings are more evenly spread among individuals within a population, usually due to limited population size resulting in higher overall mating connectivity among trees. In contrast, disassortative mating networks emerge when matings are dominated by a restricted subset of individuals, usually associated to size/fecundity hierarchies within aggregated (clustered) populations.

2.9 | Directionality of adult genetic diversity and pollen dispersal

To test for the existence of a downstream increase in population genetic diversity (i.e. the unidirectional diversity hypothesis), we compared the adult trees' expected heterozygosity (H_S) and the inbreeding coefficient (F_{IS}) between an 'upper' and a 'lower' sector of the ravine. We defined the sectors by dividing the ravine using the mean altitude in the population as a threshold for assigning each tree to its sector. We used a permutation test that randomly reassigned

individuals between groups to generate a reference distribution of test statistics to evaluate differences in H_S ($n=499$; $H_S.test$ function in the 'adegenet' package, R v.4.2.0). Additionally, we estimated F_{IS} using the *inbreeding* function in the same package and evaluated differences between sectors through ANOVA.

The directionality of pollen dispersal was assessed from paternity assignments generated by CERVUS, which allow tracking within-population movements of pollen from the source to the receptor tree. We tested the frequency of upward-downward pollen dispersal events (only considering events longer than 15 m, i.e. the average width of the riparian forest vegetation) against a random proportion of 0.5 in each direction by using a binomial test.

3 | RESULTS

3.1 | Microsatellite genotyping

All 498 candidate parents were successfully genotyped at all loci, while 12 out of the 772 analysed offspring failed to amplify and were eliminated from analyses. We recorded a total of 118 alleles in the parents (3–16 alleles per locus) and found 16 further alleles in the 760 retained seeds (Table 1). The four adult populations hardly differed in their diversity and genetic structure (only in the mean number of private alleles) despite their variable size and density (Table 1). However, the genetic diversity of progenies varied among populations, with significantly lower values in population JVEL compared to the other three populations (Tukey contrasts; $p=.0001$).

None of the population showed significant inbreeding (Table 1). All four showed spatial autocorrelation of genetic relatedness among adult trees with the intensity of spatial genetic structure (SGS) ranging between $Sp=0.011$ (PLLA) and $Sp=0.03$ (SAUC) (Table S3, Figure S3). No population showed increased SGS in the shortest distance interval (0–10 m). Furthermore, the mean kinship values within distance classes consistently remained below 0.01, with particularly lower values in population PALL.

3.2 | Effective pollen dispersal

The observed proportions of different pollination provenances (within-population, immigration, or selfing) were quite consistent among populations. By far most pollination events (92%–95%) involved fathers located within the sampled population, with a small fraction (1%–5%) originating from self-fertilization (Table 1). Relatively few events (5%–9%) were identified as originating from pollen immigration, although there was strong variation among individual mother trees (0%–27%; Table S2).

The frequency distributions of pollen dispersal distances for each of the four populations were based on 104–149 paternity assignments, respectively. All populations showed pollen dispersal curves that were leptokurtic and highly skewed to the right (Figure 1). Three of the four populations had median pollination

distances <30 m (Table 1), indicating abundant short-distance pollen flow and small genetic neighbourhoods. However, the percentage of pollination events involving distances over 100 m was sizeable (JVEL, 11%; SAUC, 23%; PLLA, 53%; and ZAPA, 37%), and the two large populations PLLA and ZAPA showed a non-negligible fraction of events exceeding 500 m (Figure 1).

3.3 | Ecological correlates of pollen dispersal and progeny diversity

We assessed ecological correlates of mating patterns using the empirical data obtained with CERVUS and several genetic estimates (Table 2). The best models (i.e. $\Delta AICc \leq 2$) for H_E , F_{IS} , Nep , and mean kinship of progeny included the null models, yet some predictor effects were also revealed. In particular, we observed that (i) larger trees tended to produce more genetically diverse progenies and to receive a disproportionately high fraction of immigration events; (ii) trees from denser neighbourhoods tended to produce progenies with a higher number of effective pollen donors and lower kinship, and to experience lower pollen dispersal distances; and (iii) trees located in the upper sector of the ravine showed slightly ($p=.09$) higher inbreeding for progenies as well as lower pollen dispersal distances.

3.4 | Spatially explicit mating models

Average estimates of mating patterns derived with MEMM showed diverse differences among populations (Table 3). The pollen dispersal parameters revealed markedly fat-tailed dispersal kernels in all populations ($b \ll 1$; range: 0.12–0.18), indicating a non-negligible potential for long-distance dispersal events. Mean dispersal distance estimates differed among populations in accordance with the spatial distribution of trees within each population. The large populations PLLA and ZAPA showed far higher estimates than SAUC and JVEL (one and two orders of magnitude, respectively). MEMM inferred a considerable amount of pollen immigration (range: 0.13–0.21) and low selfing rates (range: 0%–0.03%) in all populations. The high ratio of observed versus effective male reproductive density implied effective densities of trees between 3 and 8 times below the observed density, indicating large variance in individual fecundities (especially in ZAPA; see Table 3). This resulted in highly skewed distributions of relative fecundity in all populations, with only 12%–19% of the father trees showing relative individual male fecundities 2x above the mean population fecundity (Figure S4).

The results of the MEMM analysis allowed us to derive an adjacency matrix describing within-population patterns of mating, that is, the most likely mating events among pairs of individuals in each population. The resulting mating networks (Figure 2) appeared consistently clustered in all four study populations. Nearby individuals experienced an elevated probability of mating events, whereas ample gaps existed among clusters. This resulted in a markedly discontinuous and modular mating network for all populations, evidencing

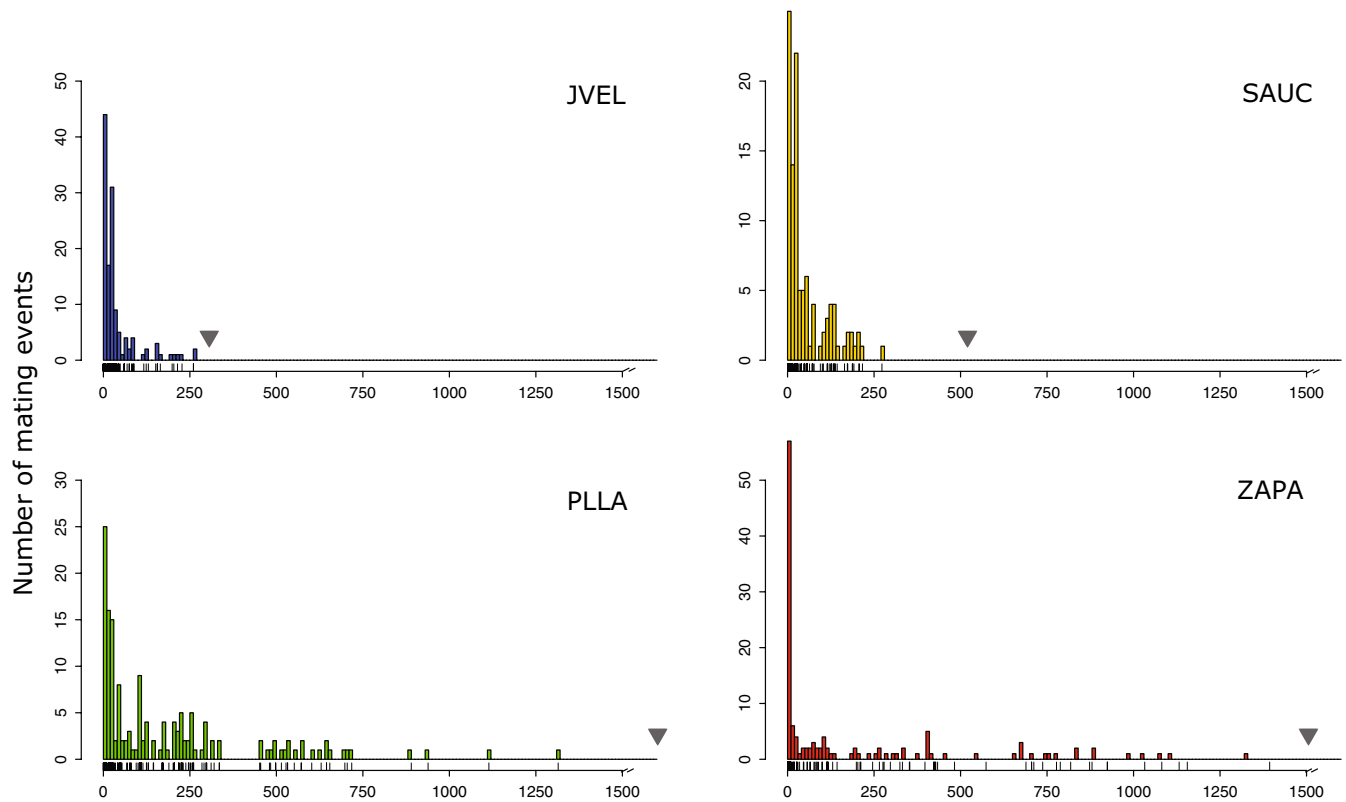


FIGURE 1 Frequency distribution of pollen dispersal distances estimated from actual mating events (CERVUS estimate) between the assigned pollen donor tree and sampled mother trees in the four *Frangula alnus* populations. The triangles indicate the stream length, that is, the maximum pollen dispersal distance within the population.

TABLE 2 Summary results of mixed-effect models to test effects of ecological variables on mating patterns in the *Frangula alnus* subsp. *baetica* populations.

Response variable	Model	AICc	Δ AICc	Weight
Gene diversity, H_E	<i>null</i>	-96.52	0.00	0.64
	~ <i>dbh</i> (+)	-94.59	1.93	0.24
Mean kinship of progeny	~ <i>rad15</i> * (-)	-87.94	0.00	0.52
	<i>null</i>	-86.20	1.75	0.22
	~ <i>rad15</i> * + <i>sector</i> (-; up<down)	-86.10	1.84	0.21
Inbreeding coefficient, F_{IS}	~ <i>sector</i> (up>down)	-79.38	0.00	0.47
	<i>null</i>	-78.83	0.54	0.36
Percent immigrants	~ <i>dbh</i> * (+)	97.21	0.00	0.59
Pollen dispersal distance (log(median))	~ <i>rad15</i> * (-)	122.11	0.00	0.51
	~ <i>rad15</i> * + <i>sector</i> (-; up<down)	123.01	0.90	0.32
Effective pollen donors, N_{ep}	<i>null</i>	349.39	0.00	0.45
	~ <i>rad15</i> (+)	350.67	1.28	0.24
	~ <i>rad15</i> + <i>dbh</i> (+; +)	351.24	1.85	0.18

Note: Predictor variables included, as fixed-effect covariates, the diameter at breast height of the focal tree (*dbh*), the number of conspecific trees within a radius of 15 m (*rad15*), and the sector of the ravine where the focal tree is located (*sector*). All models included the population as a random factor. Model selection was based on values of the Akaike Information Criterion corrected for small sampling sizes (AICc) across models with all possible factor combinations. Only the models with Δ AICc ≤ 2 were reported. Significance: * $p < .05$; ** $p < .01$; *** $p < .001$.

that some tree clusters lacked any noteworthy connection with extremely low likelihood values of mating events with other parts of the stands (Figure 2). The larger and more open populations of PLLA and

ZAPA showed a higher frequency of long-distance mating, although the most likely mating events (probability $>.05$ in Figure 2) were likewise distinctly clumped. This clumping effect is readily visualized in

TABLE 3 Summary descriptors of mating patterns and network topologies derived from MEMM simulations.

	JVEL	SAUC	PLLA	ZAPA
(A) Pollen dispersal parameters				
$d_{\text{obs}}/d_{\text{ep}}$	4.2 [2.2–7.3]	3.1 [1.3–5.9]	3.5 [1.7–6.2]	8.0 [4.3–14]
δ	48 [8–365]	141 [35–1365]	1406 [246–8674]	2277 [294–9029]
b	0.13 [0.10–0.27]	0.16 [0.10–0.44]	0.18 [0.11–0.39]	0.12 [0.10–0.20]
m	0.13 [0.10–0.18]	0.16 [0.11–0.24]	0.21 [0.14–0.29]	0.2 [0.13–0.27]
s	1.1E-7 [3.0E-25–8.7E-03]	1.2E-02 [4.7E-03–5.1E-02]	2.6E-02 [7.7E-03–5.9E-02]	9.0E-11 [1.1E-24–2.7E-03]
(B) Network-level metrics				
Connectance	0.087 [0.086–0.088]	0.047 [0.047–0.047]	0.034 [0.034–0.035]	0.021 [0.020–0.021]
Weighted connectance	0.041 [0.040–0.042]	0.028 [0.028–0.029]	0.025 [0.024–0.026]	0.017 [0.017–0.018]
NODF	11.13 [10.82–11.44]	6.99 [6.90–7.08]	5.70 [5.63–5.81]	4.29 [4.21–4.38]
Linkage density	3.229 [3.169–3.289]	4.741 [4.648–4.834]	6.560 [6.424–6.697]	7.065 [6.946–7.185]
Shannon diversity	4.522 [4.510–4.534]	5.468 [5.454–5.481]	6.147 [6.138–6.156]	6.425 [6.423–6.426]
Assortativity	0.1416	–0.0974	–0.0880	–0.1643
Modularity (no. modules)	0.69005*** (9)	0.69737*** (18)	0.79659*** (10)	0.78765*** (11)

Note: (A) Pollen dispersal parameters: Estimated ratios of observed (d_{obs}) and effective (d_{ep}) densities of male reproductive trees. Median estimates of the posterior distributions of dispersal parameters, mean dispersal distance (δ) and shape parameter of the dispersal kernel (b); as well as for the mating system parameters, migration rate (m) and selfing rate (s). The 95% credible intervals [shown in brackets] were obtained by computing the 2.5% and 97.5% quantiles from 50,000 retained values of the parameter in the MCMC simulation. (B) Network-level metrics: Connectance, weighted connectance, NODF, nestedness, linkage density, Shannon diversity, assortativity, and modularity. Significance: *** $p < .0001$.

the weighted representation of the mating networks and the corresponding weighted adjacency matrices (Figure S5). High-probability mating values distinctly occur along the adjacency matrices diagonals (Figure S5), indicative of the marked proximity effects.

All mating network metrics differed significantly among populations ($F_{3,396} > 1030$, $p < .0001$ for all among-population comparisons; Table 3, Figures S1, S5). The large populations of PLLA and ZAPA showed lower connectance and nestedness (as measured by the NODF metric) as well as higher linkage density and Shannon diversity (Table 3). Populations varied in the degree of mating network assortativity (i.e. the degree to which most linked trees tend to link to highly linked trees – i.e. positive assortativity values) or disassortativity (i.e. negative assortativity values, suggesting that low-linked trees tend to link to highly linked trees but not vice versa). Assortativity varied from positive values in the smallest population (JVEL) to higher disassortativity in the larger populations (Table 3), being positively correlated with connectance (both C and wC [$r = .974$ and $.966$, respectively, $p < .05$]) and negatively correlated with linkage density and Shannon's diversity [$r = -.880$ and $-.929$, respectively, $p < .05$]. Finally, all networks, especially the larger ones, appeared with highly clustered mating patterns, with a varying number of distinct modules (Table 3).

3.5 | Directionality of adult genetic diversity and pollen dispersal

We observed significantly higher levels of genetic diversity (H_s) in the lower than in the upper sector of two populations (JVEL and PLLA, see Table S1), consistent with the unidirectional diversity hypothesis. The other two populations showed no (SAUC) or even an

inverse (ZAPA) trend. We detected no differences in inbreeding (F_{IS}) between sectors. We found evidence of directional pollen dispersal in two of the four populations: pollen flow was preferentially downstream in JVEL and upstream in PLLA (see Table S1).

4 | DISCUSSION

4.1 | Within-population patterns of mating and pollen dispersal

We studied four *F. alnus* populations with broadly differing size and spatial structure, representative of the range of relictual conditions that the species experiences at its southernmost range limit. Our detailed empirical results, complemented by the inference of individual-level mating probabilities and resulting mating networks, allow a thorough comparison of patterns of mating and pollen dispersal in the studied populations. All of them exhibited a relatively high frequency of short-distance pollination (36%–71% within 30m of the mother tree; Figure 1), suggesting a general predominance of small genetic neighbourhoods and mating patterns with a highly structured spatial signal (Barrett & Harder, 2017). We confirmed indeed that distinct subsets of trees tending to mate among them and less likely to mate with other trees in the population (i.e. network modules or 'mating clusters') were a common phenomenon (Figure 2), especially in the larger populations. Accordingly, we observed a low network connectance and nestedness in all four populations, indicating that they lack a central core of highly and widely connected trees. This appears as a distinct feature of linearly structured, riparian tree populations along the narrow ravines that characterize our study populations. Such a modular network structure

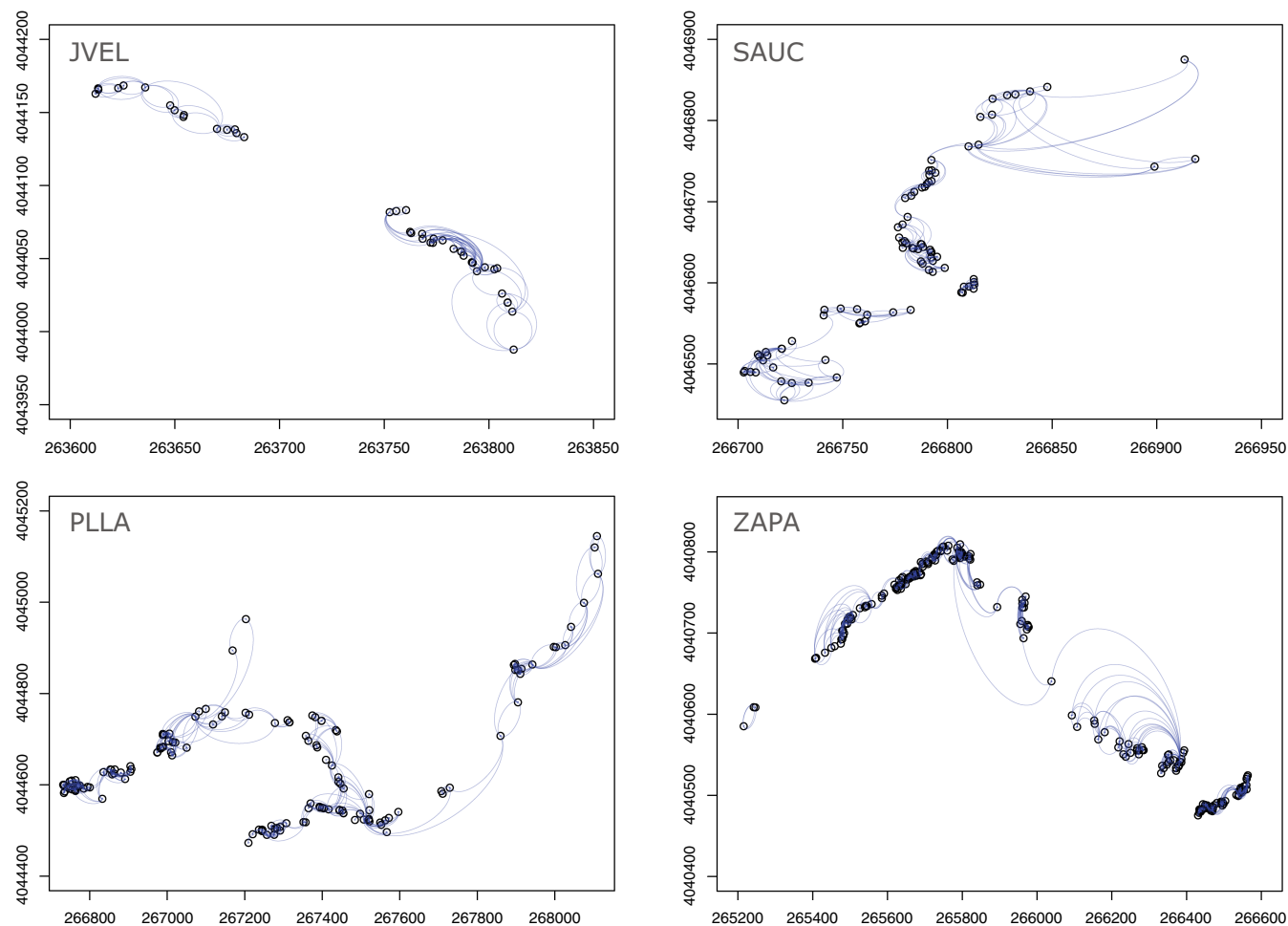


FIGURE 2 Population-wide mating networks based on the pollen dispersal kernels derived with MEMM. Circles represent individual trees, and links denote estimated mating events among the mapped individuals of each population. Each line represents a probability higher than .05 of siring events that a given mother is inferred to have from a given father. This threshold was chosen for illustrative purposes, as mating events are extremely unlikely below it. Areas concentrating likely mating events (higher density of lines in the map) are distinctly localized among closely growing trees; these mating clusters include between two to several neighbouring trees. See [Figure S5](#) for a detailed, weighted representation of the networks together with the corresponding adjacency matrices. [Colour figure can be viewed at wileyonlinelibrary.com]

would contribute to balancing fitness across individuals among spatial clusters, favouring a highly structured distribution of matings among trees (Fortuna et al., 2008; Gomez & Perfectti, 2012; Rodríguez-Rodríguez et al., 2017). The widespread existence of mating clusters is possible despite the self-incompatibility of *F. alnus* because populations experience extensive seed dispersal by avian frugivores and water flow (Hampe, 2004) that strongly reshuffles genotypes and reduces the build-up of small-scale pedigree structures. This is evidenced as no increased SGS over the shortest distance interval in [Figure S3](#).

Despite these common features, all network metrics differed significantly among populations ([Table 3](#)), revealing highly local and distinct patterns of mating, and most likely reflecting populations' ample variation in size and spatial configuration. The smallest (JVEL) and the largest (ZAPA) populations were typically the most divergent ones. The small JVEL population showed the highest network connectance and nestedness combined with the lowest modularity and Shannon diversity. This is in line with the expectation that small populations (both in terms of individuals and of

spatial extension) would tend to show pollen clouds dominated by a few individuals and relatively few structured mating networks (Meagher & Vassiliadis, 2003). In contrast, the larger populations of PLLA and ZAPA showed lower network connectance and nestedness combined with higher modularity, reflecting the presence of distinct groups of trees forming mating clusters (see, e.g. Fortuna et al., 2008). The number of mating clusters in each population resembled in fact closely the number of spatial aggregations of trees ([Figure 2](#)). It went also along with an increasing level of disassortativeness ([Table 3](#)). Disassortativeness (Newman, 2002) within mating networks is expected when matings are dominated by a few core individuals, usually due to size or fecundity hierarchies (Fortuna et al., 2008; Rodríguez-Rodríguez et al., 2017). The observed increase of disassortativeness in the larger populations, with a higher number of mating clusters suggests that, in our particular context, mating events within the spatial clusters dominate relative to those at the whole-population level. This is expected in the larger populations, where spatial aggregations of trees typically include one or a

few large individuals together with smaller trees. Highly disassortative mating patterns would thus emerge as a combination of spatial clumping, limited (highly skewed) pollen dispersal, and, eventually, size/fecundity hierarchies. Note that this type of spatially driven network disassortativeness is a priori largely independent of phenotypic variation, the most commonly investigated source of mating biases in trees and other plants (Barrett & Harder, 2017; Ismail & Kokko, 2020). In agreement with our expectation (H2), the mating networks of this riparian tree shared characteristics of marked structure and modularity, yet with (unexpectedly) ample variation among them related to population size. Only the mating network of the smallest and more isolated population showed a higher cohesiveness and less marked signal of spatial aggregation.

The analysis of ecological correlates showed that the participation (or not) of mother trees to mating clusters had direct consequences for the genetic composition of their pollen clouds. Contrary to our prediction (H1), trees from denser neighbourhoods tended to produce progenies with a higher number of effective pollen donors and lower kinship values. This trend implies that our study populations are little prone to suffering so-called 'pollen swamping', a common phenomenon in wind-pollinated species (Ouayjan & Hampe, 2018) where very few adjacent trees saturate the stigmas of their neighbours and thwart the arrival of pollen from other potential mates in the surroundings. Instead, it further pinpoints the importance of pollen limitation in the investigated populations (Hampe, 2005) that appears to act even in situations of relatively high mate density. Our findings also suggest that mother trees from high-density contexts would potentially provide the highest quality propagules for conservation and restoration programmes targeting this threatened taxon (Ferrer et al., 2011). Seed collections from adjacent trees should however be performed with caution given the observed (moderate) SGS.

Although short-distance pollen flow and the presence of mating clusters were prominent features observed in the studied populations, our analyses also revealed fat-tailed dispersal kernels with substantial pollen movements spanning hundreds of metres. Interestingly, in three out of the four populations, these pollen movements extended nearly as far as the total length of the stand permitted (Figure 2). Pollen dispersal distances increased as tree density decreased, which is consistent with other studies showing that pollinator flight distances tend to grow longer at lower plant population density (reviewed in Ghazoul, 2005; Pasquet et al., 2008). The effect should be reinforced by the linear spatial structure of the riparian populations along the gorges. This structure implies not only a reduced overall population density, but it also represents a landscape 'guide' for foraging insects that favours linear flights and the directionality of longer-distance pollen movements along the riverbed (Cranmer et al., 2012; Tewksbury et al., 2002).

4.2 | Among-population pollen dispersal

Contrary to our prediction (H3), all four isolated populations showed a noteworthy amount of pollen immigration from other *F. alnus*

populations, independently of their size and geographical isolation. The higher pollen immigration rates estimated with MEMM (13%–21%) as compared to CERVUS (5%–9%) were expected; accounting for genotyping error in CERVUS is known to artificially increase the probability of finding a compatible male within the population, despite the fact that paternity may be left unassigned (Burczyk & Chybicki, 2004). Regardless of the analytical approach, our estimates indicate that a considerable number of seeds with immigrant genotypes are produced each year, demonstrating a good potential for genetic connectivity among populations. The high amount of pollen immigration is particularly remarkable in a landscape where tree populations occur exclusively along ravines, which are enclosed and isolated by steep mountain slopes. To move between populations, pollinators must climb elevation differentials of over 100 m and/or travel some kilometres in horizontal distance – a notable physical effort and navigation challenge. Yet, we did not detect any evidence that pollen immigration would preferentially occur in the most accessible areas, either near the headwaters or near the lower ends of the gorges. Instead, trees' probability to receive immigrant pollen was determined by their size. This finding, albeit striking at first sight, is fully in line with previous field studies showing that the size and the visibility of the flower display are major drivers of seed set and fruit crop size (Hampe, 2005; Hampe & Arroyo, 2002). It indicates that trees with large floral displays are able to attract and intercept pollinators directly upon their arrival from outside the population. This ability likely also explains why large mother trees have the genetically most diverse pollen clouds (as these contain alleles from genetically distinct populations). These trees hence play a central role in the gene exchange among populations and the resulting maintenance (or recovery) of within-population genetic diversity (see also Hoshikawa et al., 2012), along with other ecological services associated with large tree size (Stephenson et al., 2014).

All but the smallest population JVLE showed low levels of genetic differentiation and moderately high to high levels of genetic diversity (Table 1). Overall, we found limited evidence that could possibly be interpreted as a consequence of their long-term fragmented distribution (Craft & Ashley, 2007). Negative genetic effects are expected when distances between isolated populations exceed the maximum dispersal distance (Bacles & Jump, 2011). Yet this is clearly not the case in the study system, even though *F. alnus* stands occur as distinctly isolated patches along ravines, separated from nearby populations by mountain ranges within a relatively restricted geographic region. Our study system thus presents one more case supporting the argumentation of Kramer et al. (2008) that tree populations may be readily connected even across major barriers in the landscape. It also presents further evidence for the potential of animal pollinators to provide regular long-distance gene flow (see also Ahmed et al., 2009), which may be even more effective in preventing long-term population isolation than wind (Moracho et al., 2016; Ouayjan & Hampe, 2018), especially when combined with animal-mediated seed dispersal (Jordano et al., 2007).

In conclusion, the observed combination of effective pollination within stands with characteristic clumping and small

neighbourhoods, and evidence of regular pollen immigration support the idea that the long-term persistence of these relict populations depends fundamentally on the interaction between the linear riverine landscape topologies and their animal-mediated dispersal mechanisms (Mari et al., 2014). This result echoes recent theoretical and experimental evidence (Altermatt, 2013) linking riverine topologies to long-term species persistence times and high local biodiversity.

4.3 | Genetic diversity and pollen dispersal along the stream

The unidirectional diversity hypothesis has received empirical support from waterborne taxa but not from plants (Honnay et al., 2010; Paz-Viñas et al., 2015). It is hence intriguing that two out of our four populations (JVEL and PLLA) exhibited a significant increase of genetic diversity (H_s) downstream over distances of just a few hundred metres, and inbreeding levels of our progenies tended to decrease downstream (Table 2), thereby supporting our hypothesis (H4). The long-term stability and considerable waterborne seed dispersal in our study system, are likely to contribute to these trends. However, other factors may blur the expected downstream increase in genetic diversity as observed in other populations, such as fat-tailed pollen dispersal kernels, preferential upstream pollen dispersal (as a consequence of pollinator behaviour), and preferential pollen immigration near the headwaters (see also Hoshikawa et al., 2012). First, all four populations exhibited fat-tailed dispersal kernels, with population ZAPA in particular having the lowest proportion of long-distance pollen dispersal (Figure 2). Second, directional pollen dispersal does not appear to play a major role in longitudinal genetic diversity trends as not a consistent trend was observed in our populations. Finally, there was no evidence to suggest a preferential occurrence of pollen immigration near the headwaters. Therefore, observed pollen dispersal patterns cannot account alone for the differing spatial trends in genetic diversity. In addition, differences in seed dispersal and other processes, such as bird-mediated upstream seed dispersal or higher recruitment success near headwaters, are likely to importantly contribute to shaping the genetic structure of riparian tree populations (see also Honnay et al., 2010).

5 | CONCLUSION

Habitat fragmentation is a global phenomenon that affects numerous tree species, but its consequences for the genetic structure and diversity of tree populations are diverse and complex (Bacles & Jump, 2011; Kramer et al., 2008). Through our detailed individual-based analyses of mating and gene flow patterns, we provide compelling evidence of the ecological mechanisms that enable naturally fragmented riparian tree populations to maintain their genetic diversity over extended periods of time. On the one hand, frequent

short-distance pollen flow and small genetic neighbourhoods prevent populations' genetic composition from being dominated by a few highly fecund trees. On the other hand, surprisingly common inter-population pollen dispersal limits the effective isolation of populations. Our study also reveals the interesting and novel finding that although the mating systems of the four populations were relatively similar, their mating network topologies varied considerably (e.g. the frequency and density of mating events, locally structured matings). These insights into the complex and highly structured reproduction in these relict tree populations (including the role of dense tree groups forming mating clusters or the contribution of large trees as 'traps' for immigrant pollen) represent valuable baseline information for ongoing conservation and restoration initiatives (Ferrer et al., 2011).

In their comprehensive review, Blanchet et al. (2020) highlighted that the study of within-species genetic diversity in riverscapes has received considerably less attention compared to terrestrial systems, and it is rarely the target of global conservation policies. Our study illustrates how carefully designed research can shed light on the particularities of riparian taxa and provide valuable insights for developing effective conservation strategies in a rapidly changing world.

AUTHOR CONTRIBUTIONS

E.M., A.H., and P.J. conceived the study. E.M. and S.O.M. carried out data curation. E.M. and P.J. supervised laboratory work. E.M., E.K., S.O.M., and P.J. analysed data. E.M. lead writing. E.M., A.H., and P.J. wrote the final version. S.O.M. contributed in interpreting results and final manuscript edition.

ACKNOWLEDGEMENTS

This work would have not been possible without the dedicated technical support provided by Juan Miguel Arroyo, Manuel Carrión, and Cristina Rigueiro. We are grateful to Rocío Rodríguez for her invaluable assistance with fieldwork, lab analysis, and comments on early drafts of the manuscript, as well as to Alberto Roldán for his help with field work. PJ and EM are funded by the Spanish Ministry of Science, Innovation, and Universities (grants CGL2010-18381 and PID2022-136812NB-I00) and LifeWatch ERIC-SUMHAL (LIFEWATCH-2019-09-CSIC-13)/FEDER-EU funding, and the VI and VII Research Funding Program from Universidad de Sevilla (2021/00000826). We appreciate the assistance of the Doñana ICTS Monitoring Team of Estación Biológica de Doñana, and the LAST facilities (David Aragonés) for enabling the analysis of satellite images and helping with georeferencing. The Consejería de Medio Ambiente provided permits and facilities to conduct our field work in Parque Natural de Los Alcornocales, Cádiz.

CONFLICT OF INTEREST STATEMENT

Authors declare no conflicts of interest for this article.

DATA AVAILABILITY STATEMENT

The data that support the findings of this study are openly available in GitHub (https://github.com/PJordano-Lab/MS_MolEcol_

Frangula) and DRYAD [<https://doi.org/10.5061/dryad.9p8cz8wq1>] [doi: 10.5061/dryad.9p8cz8wq1].

ORCID

Etienne K. Klein  <https://orcid.org/0000-0003-4677-0775>

Pedro Jordano  <https://orcid.org/0000-0003-2142-9116>

REFERENCES

- Aguilar, R., Cristóbal-Pérez, E. J., Balvino-Olvera, F. J., de Jesús Aguilar-Aguilar, M., Aguirre-Acosta, N., Ashworth, L., Lobo, J. A., Martén-Rodríguez, S., Fuchs, E. J., Sanchez-Montoya, G., Bernardello, G., & Quesada, M. (2019). Habitat fragmentation reduces plant progeny quality: A global synthesis. *Ecology Letters*, 22, 1163–1173.
- Aguilar, R., Quesada, M., Ashworth, L., Herrerias-Diego, Y., & Lobo, J. (2008). Genetic consequences of habitat fragmentation in plant populations: Susceptible signals in plant traits and methodological approaches. *Molecular Ecology*, 17, 5177–5188.
- Ahmed, S., Compton, S. G., Butlin, R. K., & Gilmartin, P. M. (2009). Windborne insects mediate directional pollen transfer between desert fig trees 160 kilometers apart. *Proceedings of the National Academy of Sciences of the United States of America*, 106, 20342–20347.
- Albert, R., & Barabási, A. L. (2002). Statistical mechanics of complex networks. *Reviews of Modern Physics*, 74, 47–97.
- Altermatt, F. (2013). Diversity in riverine metacommunities: A network perspective. *Aquatic Ecology*, 47, 365–377.
- Anderson, D. R., & Burnham, K. P. (2002). Avoiding pitfalls when using information-theoretic methods. *The Journal of Wildlife Management*, 66, 912–918.
- Bacles, C., & Jump, A. (2011). Taking a tree's perspective on forest fragmentation genetics. *Trends in Plant Science*, 16, 13–18.
- Baguette, M., Blanchet, S., Legrand, D., Stevens, V. M., & Turlure, C. (2013). Individual dispersal, landscape connectivity and ecological networks. *Biological Reviews*, 88, 310–326.
- Barabási, A. L., & Pósfai, M. (2016). *Network science*. Cambridge University Press.
- Barrett, S. C., & Harder, L. D. (2017). The ecology of mating and its evolutionary consequences in seed plants. *Annual Review of Ecology, Evolution, and Systematics*, 48, 135–157.
- Bascompte, J., Jordano, P., Melián, C. J., & Olesen, J. M. (2003). The nested assembly of plant-animal mutualistic networks. *Proceedings of the National Academy of Sciences of the United States of America*, 100, 9383–9387.
- Bersier, L. F., Banašek-Richter, C., & Cattin, M. F. (2002). Quantitative descriptors of food-web matrices. *Ecology*, 83, 2394–2407.
- Bertolasi, B., Leonarduzzi, C., Piotti, A., Leonardi, S., Zago, L., Gui, L., Gorian, F., Vanetti, I., & Binelli, G. (2015). A last stand in the Po valley: Genetic structure and gene flow patterns in *Ulmus minor* and *U. pumila*. *Annals of Botany*, 115, 683–692.
- Blanchet, S., Prunier, J. G., Paz-Vinas, I., Saint-Pé, K., Rey, O., Raffard, A., Mathieu-Bégné, E., Loot, G., Fourtune, L., & Dubut, V. (2020). A river runs through it: The causes, consequences, and management of intraspecific diversity in river networks. *Evolutionary Applications*, 13, 1195–1213.
- Burczyk, J., & Chybicki, I. J. (2004). Cautions on direct gene flow estimation in plant populations. *Evolution*, 58, 956–963.
- Craft, K., & Ashley, M. (2007). Landscape genetic structure of bur oak (*Quercus macrocarpa*) savannas in Illinois. *Forest Ecology and Management*, 239, 13–20.
- Cranmer, L., McCollin, D., & Ollerton, J. (2012). Landscape structure influences pollinator movements and directly affects plant reproductive success. *Oikos*, 121, 562–568.
- Cushman, S. A., Max, T., Meneses, N., Evans, L. M., Ferrier, S., Honchak, B., Whitham, T. G., & Allan, G. J. (2014). Landscape genetic connectivity in a riparian foundation tree is jointly driven by climatic gradients and river networks. *Ecological Applications*, 24, 1000–1014.
- Dudgeon, D., Arthington, A. H., Gessner, M. O., Kawabata, Z. I., Knowler, D. J., Lévêque, C., Naiman, R. J., Prieur-Richard, A. H., Soto, D., Stiassny, M. L. J., & Sullivan, C. A. (2006). Freshwater biodiversity: Importance, threats, status and conservation challenges. *Biological Reviews*, 81, 163–182.
- Dyer, R. J. (2015). Population graphs and landscape genetics. *Annual Review of Ecology, Evolution, and Systematics*, 46, 327–342.
- Ferrer, P., Albert, F., Arregui, J. M., ..., Laguna, E. (2011). *Frangula alnus* subsp. *baetica*: conservación en la Comunidad Valenciana. *Conservación Vegetal*, 15, 14–15.
- Fortuna, M. A., García, C., Guimaraes Jr., P. R. & Bascompte, J. (2008). Spatial mating networks in insect-pollinated plants. *Ecology Letters*, 11, 490–498.
- Ghazoul, J. (2005). Pollen and seed dispersal among dispersed plants. *Biological Reviews*, 80, 413–443.
- Gomez, J. M., & Perfectti, F. (2012). Fitness consequences of centrality in mutualistic individual-based networks. *Proceedings of the Royal Society B: Biological Sciences*, 279, 1754–1760.
- Goto, S., Shimatani, K., Yoshimaru, H., & Takahashi, Y. (2006). Fat-tailed gene flow in the dioecious canopy tree species *Fraxinus mandshurica* var. *japonica* revealed by microsatellites. *Molecular Ecology*, 15, 2985–2996.
- Goudet, J. (1995). FSTAT (version 1.2): A computer program to calculate F-statistics. *Journal of Heredity*, 86, 485–486.
- Grill, G., Lehner, B., Thieme, M., Geenen, B., Tickner, D., Antonelli, F., Babu, S., Borrelli, P., Cheng, L., Crochetiere, H., Ehalt Macedo, H., Filgueiras, R., Goichot, M., Higgins, J., Hogan, Z., Lip, B., McClain, M. E., Meng, J., Mulligan, M., ... Zarfl, C. (2019). Mapping the world's free-flowing rivers. *Nature*, 569, 215–221.
- Haddad, N. M., Brudvig, L. A., Clobert, J., Davies, K. F., Gonzalez, A., Holt, R. D., Lovejoy, T. E., Sexton, J. O., Austin, M. P., Collins, C. D., Cook, W. M., Damschen, E. I., Ewers, R. M., Foster, B. L., Jenkins, C. N., King, A. J., Lurance, W. F., Levey, D. J., Margules, C. R., ... Townshend, J. R. (2015). Habitat fragmentation and its lasting impact on Earth's ecosystems. *Science Advances*, 1, e1500052.
- Hampe, A. (2004). Extensive hydrochory uncouples spatiotemporal patterns of seedfall and seedling recruitment in a "bird-dispersed" riparian tree. *Journal of Ecology*, 92, 797–807.
- Hampe, A. (2005). Fecundity limits in *Frangula alnus* (Rhamnaceae) relict populations at the species' southern range margin. *Oecologia*, 143, 377–386.
- Hampe, A., & Arroyo, J. (2002). Recruitment and regeneration in populations of an endangered south Iberian tertiary relict tree. *Biological Conservation*, 107, 263–271.
- Hampe, A., Arroyo, J., Jordano, P., & Petit, R. J. (2003). Rangelwide phylogeography of a bird-dispersed Eurasian shrub: Contrasting Mediterranean and temperate glacial refugia. *Molecular Ecology*, 12, 3415–3426.
- Hardy, O. J., & Vekemans, X. (2002). SPAGEDi: A versatile computer program to analyse spatial genetic structure at the individual or population levels. *Molecular Ecology Notes*, 2, 618–620.
- Honnay, O., Jacquemyn, H., Nackaerts, K., Breyne, P., & Van Looy, K. (2010). Patterns of population genetic diversity in riparian and aquatic plant species along rivers. *Journal of Biogeography*, 37, 1730–1739.
- Hoshikawa, T., Nagamitsu, T., & Tomaru, N. (2012). Effects of pollen availability on pollen immigration and pollen donor diversity in riparian dioecious trees (*Salix arbutifolia*). *Botany*, 90, 481–489.
- Ismail, S. A., & Kokko, H. (2020). An analysis of mating biases in trees. *Molecular Ecology*, 29, 184–198.
- Jordano, P., Garcia, C., Godoy, J. A., & Garcia-Castaño, J. (2007). Differential contribution of frugivores to complex seed dispersal patterns. *Proceedings of the National Academy of Sciences of the United States of America*, 104, 3278–3282.

- Kalinowski, S. T., Taper, M. L., & Marshall, T. C. (2007). Revising how the computer program CERVUS accommodates genotyping error increases success in paternity assignment. *Molecular Ecology*, *16*, 1099–1106.
- Kalinowski, S. T., Wagner, A. P., & Taper, M. L. (2006). ML-relate: A computer program for maximum likelihood estimation of relatedness and relationship. *Molecular Ecology Notes*, *6*, 576–579.
- Klein, E. K., Desassis, N., & Oddou-Muratorio, S. (2008). Pollen flow in the wild service tree, *Sorbus torminalis* (L.) Crantz. IV. Whole interindividual variance of male fecundity estimated jointly with the dispersal kernel. *Molecular Ecology*, *17*, 3323–3336.
- Kramer, A. T., Ison, J. L., Ashley, M. V., & Howe, H. F. (2008). The paradox of forest fragmentation genetics. *Conservation Biology*, *22*, 878–885.
- Kremer, A., Ronce, O., Robledo-Arnuncio, J. J., Guillaume, F., Bohrer, G., Nathan, R., Bridle, J. R., Gomulkiewicz, R., Klein, E. K., Ritland, K., Kuparinen, A., Gerber, S., & Schueler, S. (2012). Long-distance gene flow and adaptation of forest trees to rapid climate change. *Ecology Letters*, *15*, 378–392.
- Lindenmayer, D. B., & Fischer, J. (2013). *Habitat fragmentation and landscape change: An ecological and conservation synthesis*. Island Press.
- Loiselle, B. A., Sork, V. L., Nason, J., & Graham, C. (1995). Spatial genetic structure of a tropical understory shrub, *Psychotria officinalis* (Rubiaceae). *American Journal of Botany*, *82*, 1420–1425.
- Manoel, R. O., Freitas, M. L. M., Furlani, E., Alves, P. F., Moraes, M. L. T., & Sebbenn, A. M. (2017). Low levels of pollen and seed flow in a riparian forest fragment of the dioecious tropical tree *Genipa americana* L. *Forestry Research and Engineering: International Journal*, *1*, 00003.
- Mari, L., Casagrandi, R., Bertuzzo, E., Rinaldo, A., & Gatto, M. (2014). Metapopulation persistence and species spread in river networks. *Ecology Letters*, *17*, 426–434.
- Marshall, T. C., Slate, J., Kruuk, L. E. B., & Pemberton, J. M. (1998). Statistical confidence for likelihood-based paternity inference in natural populations. *Molecular Ecology*, *7*, 639–655. doi: [10.1046/j.1365-294x.1998.00374.x](https://doi.org/10.1046/j.1365-294x.1998.00374.x)
- Mazerolle, M. J. (2020). AICcmodavg: Model selection and multimodel inference based on (Q)AIC(c). R package version 2.3-1. <https://cran.r-project.org/package=AICcmodavg>
- Meagher, T. R., & Vassiliadis, C. (2003). Spatial geometry determines gene flow in plant populations. In 'Genes in the Environment'. *The Fifteenth Special Symposium of the British Ecological Society*. Oxford, UK.
- Medan, D. (1994). Reproductive biology of *Frangula alnus* (Rhamnaceae) in southern Spain. *Plant Systematics and Evolution*, *193*, 173–186.
- Meusel, H., et al. (1978). *Vergleichende Chorologie der zentralen europäischen Flora*, Vol. 2. Fischer.
- Milligan, B. G. (1998). Total DNA isolation. In A. R. Hoelzel (Ed.), *Molecular genetic analysis of populations: A practical approach* (2nd ed., pp. 3–44). Oxford University Press.
- Moracho, E., Moreno, G., Jordano, P., & Hampe, A. (2016). Unusually limited pollen dispersal and connectivity of pedunculate oak (*Quercus robur*) refugial populations at the species' southern range margin. *Molecular Ecology*, *25*, 3319–3331.
- Nakagawa, S., & Schielzeth, H. (2013). A general and simple method for obtaining R^2 from generalized linear mixed-effects models. *Methods in Ecology and Evolution*, *4*, 133–142.
- Newman, M. (2002). Assortative mixing in networks. *Physical Review Letters*, *89*, 208701.
- Oddou-Muratorio, S., Houot, M. L., Demesure-Musch, B., & Austerlitz, F. (2003). Pollen flow in the wild service tree, *Sorbus torminalis* (L.) Crantz. I. Evaluating the paternity analysis procedure in continuous populations. *Molecular Ecology*, *12*, 3427–3439.
- Oksanen, J., Blanchet, F. G., Kindt, R., et al. (2013). vegan: Community Ecology Package. R package version 2.0-8. <http://CRAN.R-project.org/package=vegan>
- Olesen, J. M., Bascompte, J., Dupont, Y. L., & Jordano, P. (2007). The modularity of pollination networks. *Proceedings of the National Academy of Sciences of the United States of America*, *104*, 19891–19896.
- Ouayan, A., & Hampe, A. (2018). Extensive sib-mating in a refugial population of beech (*Fagus sylvatica*) growing along a lowland river. *Forest Ecology and Management*, *407*, 66–74.
- Paradis, E., Baillie, S. R., & Sutherland, W. J. (2002). Modeling large-scale dispersal distances. *Ecological Modelling*, *151*, 279–292.
- Pasquet, R. S., Peltier, A., Hufford, M. B., Oudin, E., Saulnier, J., Paul, L., Knudsen, J. T., Herren, H. R., & Gepts, P. (2008). Long-distance pollen flow assessment through evaluation of pollinator foraging range suggests transgene escape distances. *Proceedings of the National Academy of Sciences of the United States of America*, *105*, 13456–13461.
- Paz-Viñas, I., Loot, G., Stevens, V. M., & Blanchet, S. (2015). Evolutionary processes driving spatial patterns of intraspecific genetic diversity in river ecosystems. *Molecular Ecology*, *24*, 4586–4604.
- Petit, R. J., & Hampe, A. (2006). Some evolutionary consequences of being a tree. *Annual Review of Ecology, Evolution, and Systematics*, *37*, 187–214.
- R Development Core Team. (2022). *R: A Language and Environment for Statistical Computing*. R Foundation for Statistical Computing Vienna, Austria. <https://www.R-project.org/>
- Rigueiro, C., Arroyo, J. M., Rodríguez, R., Hampe, A., & Jordano, P. (2009). Isolation and characterization of 16 polymorphic microsatellite loci for *Frangula alnus* (Rhamnaceae). *Molecular Ecology Resources*, *9*, 986–989.
- Rodríguez-Rodríguez, M. C., Jordano, P., & Valido, A. (2017). Functional consequences of plant-animal interactions along the mutualism-antagonism gradient. *Ecology*, *98*, 1266–1276.
- Rodríguez-Sánchez, F., Pérez-Barrales, R., Ojeda, F., Vargas, P., & Arroyo, J. (2008). The strait of Gibraltar as a melting pot for plant biodiversity. *Quaternary Science Reviews*, *27*, 2100–2117.
- Sarker, S., Veremyev, A., Boginski, V., & Singh, A. (2019). Critical nodes in river networks. *Scientific Reports*, *9*, 11178.
- Stephenson, N. L., Das, A. J., Condit, R., et al. (2014). Rate of tree carbon accumulation increases continuously with tree size. *Nature*, *507*, 90–93.
- Tewksbury, J. J., Levey, D. J., Haddad, N. M., Sargent, S., Orrock, J. L., Weldon, A., Danielson, B. J., Brinkerhoff, J., Damschen, E. I., & Townsend, P. (2002). Corridors affect plants, animals, and their interactions in fragmented landscapes. *Proceedings of the National Academy of Sciences of the United States of America*, *99*, 12923–12926.
- Tonnabel, J., Klein, E. K., Ronce, O., Oddou-Muratorio, S., Rousset, F., Olivieri, I., Courtiol, A., & Mignot, A. (2021). Sex-specific spatial variation in fitness in the highly dimorphic *Leucadendron rubrum*. *Molecular Ecology*, *30*, 1721–1735.
- Weir, B. S., & Goudet, J. (2017). A unified characterization of population structure and relatedness. *Genetics*, *206*, 2085–2103. doi: [10.1534/genetics.116.198424](https://doi.org/10.1534/genetics.116.198424)
- Werth, S., & Scheidegger, C. (2014). Gene flow within and between catchments in the threatened riparian plant *Myricaria germanica*. *PLoS One*, *9*, e99400.
- Young, A. G., & Clarke, G. M. (2000). *Genetics, demography and viability of fragmented populations*. Cambridge University Press.

SUPPORTING INFORMATION

Additional supporting information can be found online in the Supporting Information section at the end of this article.

How to cite this article: Moracho, E., Klein, E. K., Oddou-Muratorio, S., Hampe, A., & Jordano, P. (2024). Highly clustered mating networks in naturally fragmented riparian tree populations. *Molecular Ecology*, *33*, e17285. <https://doi.org/10.1111/mec.17285>

Supplementary Material

Highly clustered mating networks in naturally-fragmented riparian tree populations

E. Moracho^{1*}, E. Klein^{2,3}, S. Oddou-Muratorio², A. Hampe^{4,5} & P. Jordano^{1,6}

¹ Integrative Ecology Group, Estación Biológica de Doñana (EBD-CSIC), Av. Américo Vespucio 26, Isla de la Cartuja, E-41092 Sevilla, Spain

² Ecologie des Forêts Méditerranéennes, UR 629, INRA, F-84914 Avignon cedex 9, France

³ Biostatistique et Processus Spatiaux, UR 546, INRA, F-84914 Avignon cedex 9, France

⁴ INRA, UMR1202 BIOGECO, F-33610 Cestas, France

⁵ Univ. Bordeaux, UMR1202 BIOGECO, F-33400 Talence, France

⁶ Dept. Biología Vegetal y Ecología, Universidad de Sevilla, Av. Reina Mercedes s/n, Sevilla, Spain

Table S1. Directionality in genetic diversity of adult trees and pollen dispersal in ravines. Directionality is defined as upward (upw.) or downward (downw.) within the ravine, and as such, the analysis was based on differentiating between an 'upper sector' and a 'lower sector'.

The analysis of the directionality of genetic diversity includes two parameters, expected heterozygosity (H_s) and the inbreeding coefficient of individuals (F_{IS}). Differences in expected heterozygosity were evaluated by randomly permuting individuals between groups to obtain a reference distribution of the test statistics ($n=499$) using *Hs.test* in package 'adegenet' (R v.4.2.0). F_{IS} was estimated by computing its likelihood function using function *inbreeding* in the 'adegenet' package. ANOVA was used to test differences in inbreeding among populations.

To test the directionality of pollen dispersal (deviations from random events upward and downward the streams), we used known paternities within the population assigned by CERVUS. We analyzed the frequencies of pollen dispersal events (distances over 15 m) in upward or downward directions and tested them against a random proportion of 0.5 in each direction by using a binomial test.

	JVEL			SAUC			PLLA			ZAPA		
A. Genetic diversity	Upper	Lower	P									
H_s	0.338	0.449	0.024	0.505	0.485	ns	0.490	0.525	0.008	0.485	0.462	0.006
F_{IS}	0.221	0.255	ns	0.190	0.223	ns	0.211	0.208	ns	0.205	0.211	ns
B. Pollen dispersal	Upw.	Downw.	P									
No. of events	28	44	0.076	35	36	0.934	76	50	0.026	31	38	0.47

Table S2. Mother plants used as biological pollen traps in four *Frangula* populations. Sector indicates the part of the ravine where sampled trees are located (classified as upperstream or downstream). Density indicates the number of adult conspecifics within a radius of 15 m of each mother tree. Paternity assignment, estimated with CERVUS at 95% confidence level, can result, for each individual seed, in either a uniquely identified pollen donor (which can be the mother tree itself, indicated as selfing), an unresolved paternity with more than one possible pollen donor (indicated as unassigned), or all trees in the population being excluded as potential pollen donors (paternity assigned to immigrant pollen). The numbers indicate the number of observed cases with the percentage in parentheses.

	Mother	Sector	Density	No. embryos genotyped	No. pollen donors	Assigned	Unassigned	Selfing	Immigration
JVEL	JV0605	upper	10	30	12	15 (50)	12 (40)	2 (7)	1 (3)
	JV0607	upper	8	30	14	19 (63)	10 (33)	0 (0)	1 (3)
	JV0612	lower	3	30	10	14 (47)	13 (43)	1 (3)	2 (7)
	JV0624	lower	4	25	10	24 (96)	1 (4)	0 (0)	0 (0)
	JV0786	upper	1	30	9	13 (43)	9 (30)	4 (13)	4 (13)
	JV0787	upper	5	30	10	13 (43)	12 (40)	3 (10)	2 (7)
	JV0853	lower	5	30	6	22 (73)	6 (20)	0 (0)	2 (7)
SAUC	4S0164	upper	7	14	9	12 (86)	0 (0)	0 (0)	2 (14)
	4S0169	upper	3	15	9	14 (93)	0 (0)	0 (0)	1 (7)
	4S0189	upper	8	15	11	12 (80)	0 (0)	0 (0)	3 (20)
	4S0197	upper	8	14	14	13 (93)	0 (0)	0 (0)	1 (7)
	4S0211	lower	6	15	11	14 (93)	0 (0)	0 (0)	1 (7)
	4S0229	lower	2	15	3	13 (87)	0 (0)	2 (13)	0 (0)
	4S0232	lower	3	15	6	14 (93)	0 (0)	0 (0)	1 (7)
	4S0238	lower	1	14	10	12 (86)	0 (0)	1 (7)	1 (7)
PLLA	S0043	lower	1	15	9	9 (90)	0 (0)	0 (0)	1 (10)
	S0073	lower	2	14	10	12 (86)	0 (0)	1 (7)	1 (7)
	S0075	upper	4	14	7	13 (93)	0 (0)	0 (0)	1 (7)
	S0079	upper	7	15	10	15 (100)	0 (0)	0 (0)	0 (0)
	S0088	lower	4	15	12	13 (87)	0 (0)	0 (0)	2 (13)
	S0094	upper	2	15	9	15 (100)	0 (0)	0 (0)	0 (0)
	S0109	upper	2	15	7	10 (91)	0 (0)	1 (9)	0 (0)
	S0151	lower	2	14	12	12 (86)	0 (0)	0 (0)	2 (14)
	S0157	lower	1	15	13	8 (53)	0 (0)	3 (20)	4 (27)
	S0867	upper	4	15	12	13 (87)	0 (0)	0 (0)	2 (13)
	S0868	upper	1	14	10	14 (100)	0 (0)	0 (0)	0 (0)
	S0870	upper	7	15	7	15 (100)	0 (0)	0 (0)	0 (0)
ZAPA	Z0357	lower	3	15	12	12 (80)	1 (7)	0 (0)	2 (13)
	Z0377	lower	5	15	8	12 (80)	1 (7)	1 (7)	1 (7)
	Z0386	upper	2	15	10	13 (87)	2 (13)	0 (0)	0 (0)
	Z0562b	lower	3	30	17	17 (57)	11 (37)	0 (0)	2 (7)
	Z0598	lower	20	15	10	13 (87)	1 (7)	0 (0)	1 (7)
	Z0762	upper	13	28	9	23 (82)	4 (14)	0 (0)	1 (4)
	Z0765	upper	15	29	5	27 (93)	2 (7)	0 (0)	0 (0)
	Z0776	upper	12	15	8	10 (67)	4 (27)	0 (0)	1 (7)

Table S3. Estimate of spatial genetic structure (SGS) and inbreeding (F) for each population.

The S_p statistics expresses the strength of the SGS, and was computed from the average kinship coefficient between individuals separated by less than 10 m (F_{10}), and $b_{\log F}$.

Standard errors (SE) are given in brackets.

	F10 (SE)	$b_{\log F}$ (SE)	S_p (SE)	F (SE)
JVEL	0.046 (0.018)	-0.022 (0.008)	0.023 (0.008)	0.024 (0.036)
PPLA	0.009 (0.006)	-0.011 (0.003)	0.011 (0.003)	0.015 (0.023)
SAUC	0.072 (0.015)	-0.028 (0.007)	0.03 (0.007)	0.044 (0.027)
ZAPA	0.043 (0.007)	-0.014 (0.002)	0.015 (0.002)	0.027 (0.016)

Figure S1. Location and size of adult trees in the four studied *F. alnus* populations. Circle size indicates the diameter at breast height (dbh) of the tree. Highlighted circles indicate the mother plants from which we collected fruits for the parent-offspring genetic analyses. Scale (whole bar) is 100 m.

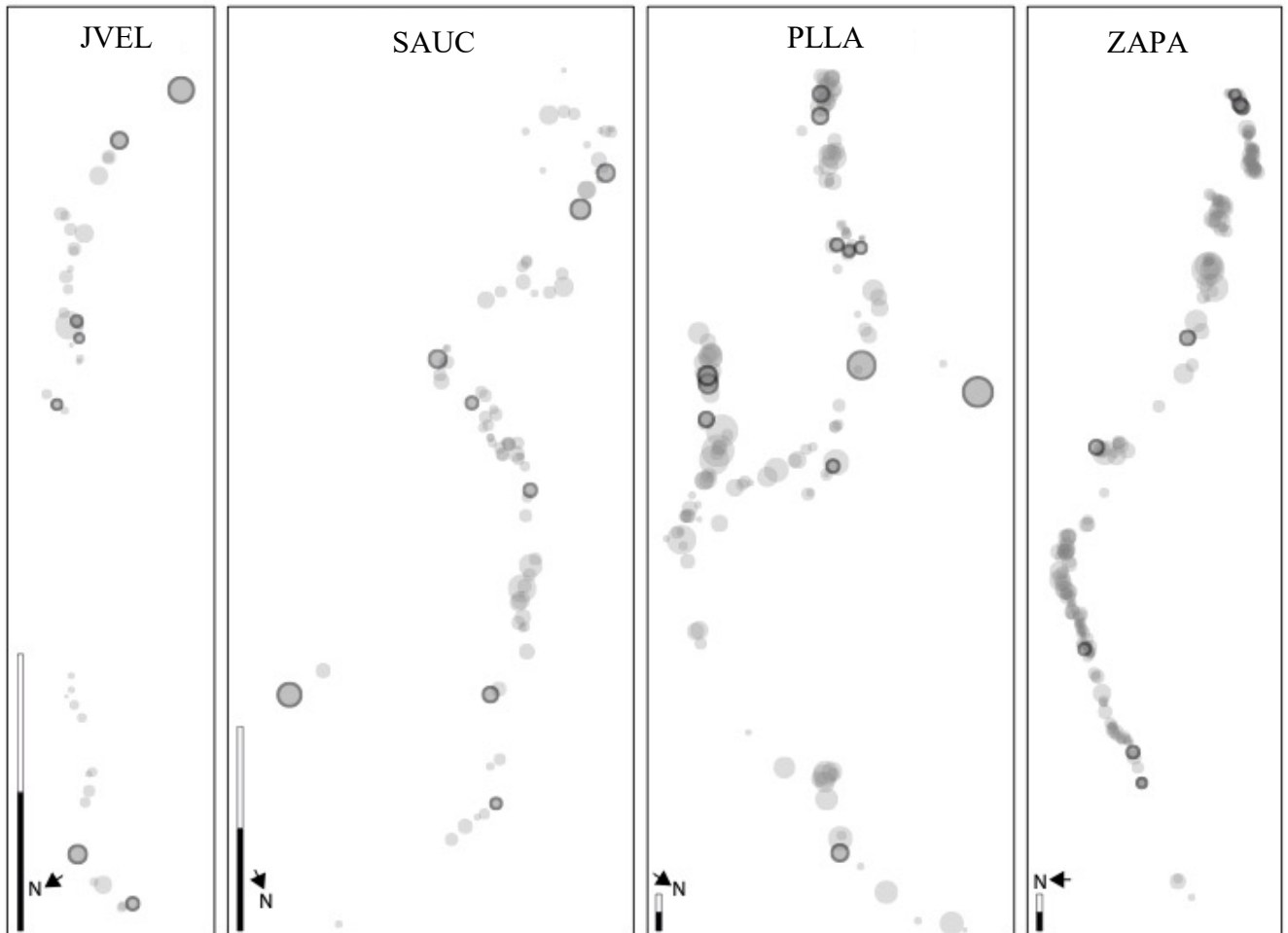


Figure S2. Genetic diversity accumulation curves for embryo progenies sampled in JVEL population. Each panel corresponds to one mother tree.

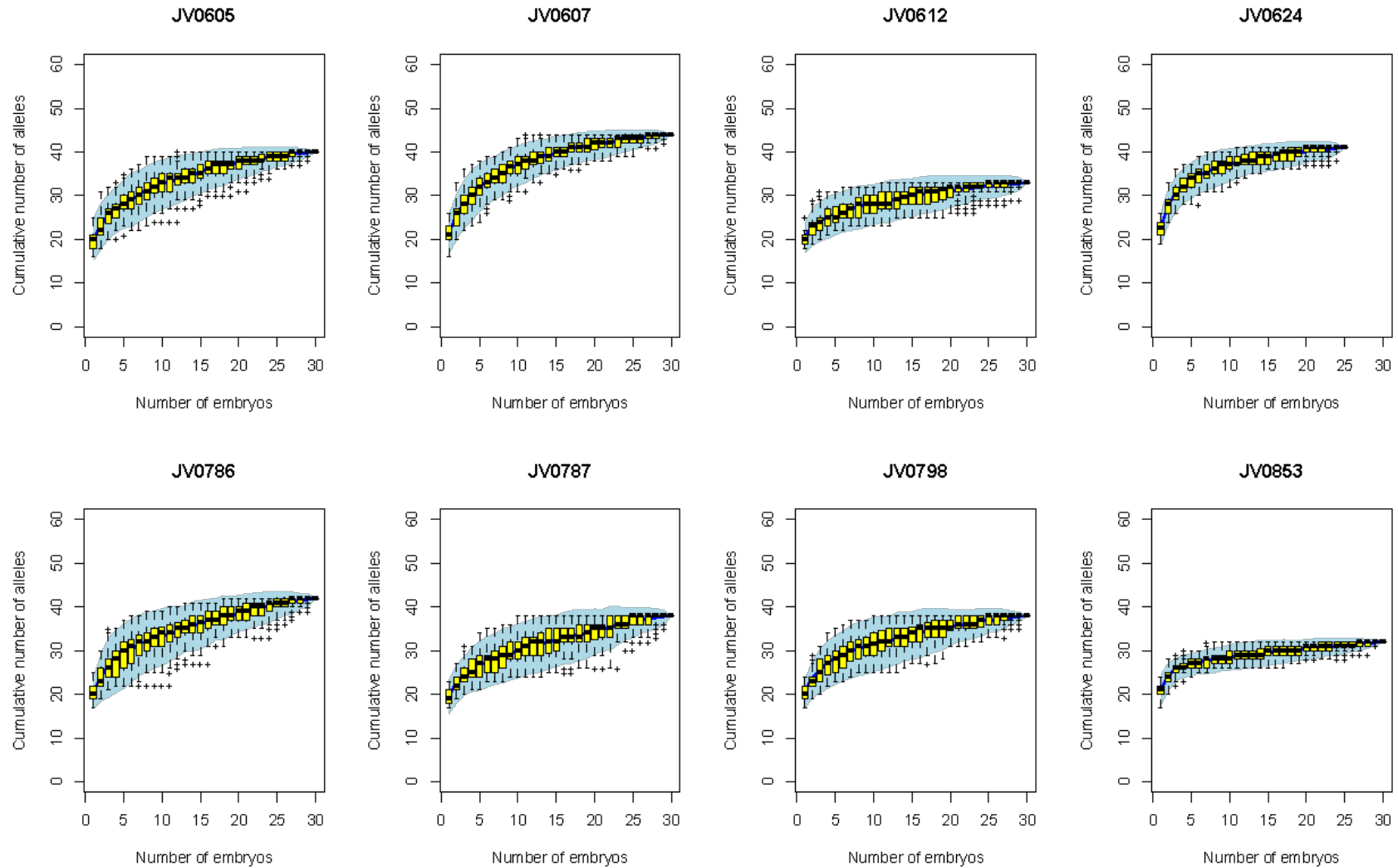


Figure S3. Spatial autocorrelation of kinship coefficients computed for the adult trees of the four populations. Filled symbols represent values significantly different from the expected value under a random distribution of genotypes (95% confidence level). Confidence intervals around each F_{ij} value were obtained through a jackknife procedure over loci.

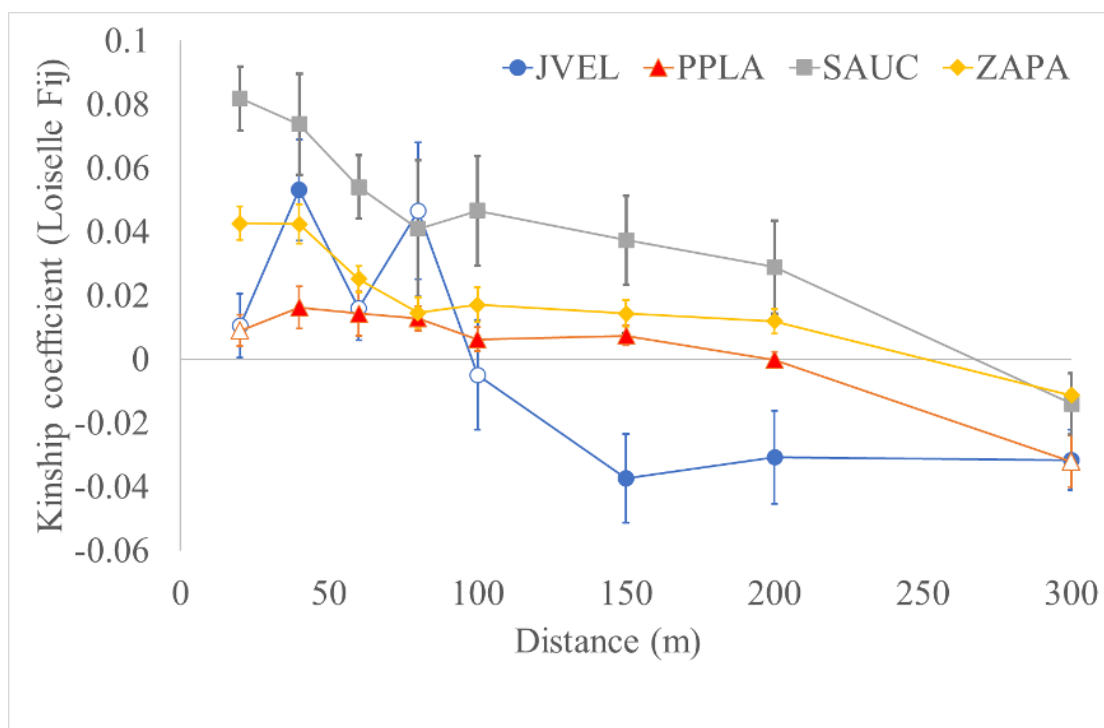


Figure S4. Distribution of individual relative male fecundities, estimated through a Bayesian approach implemented in MEMM, for all trees growing in the four *F. alnus* populations.

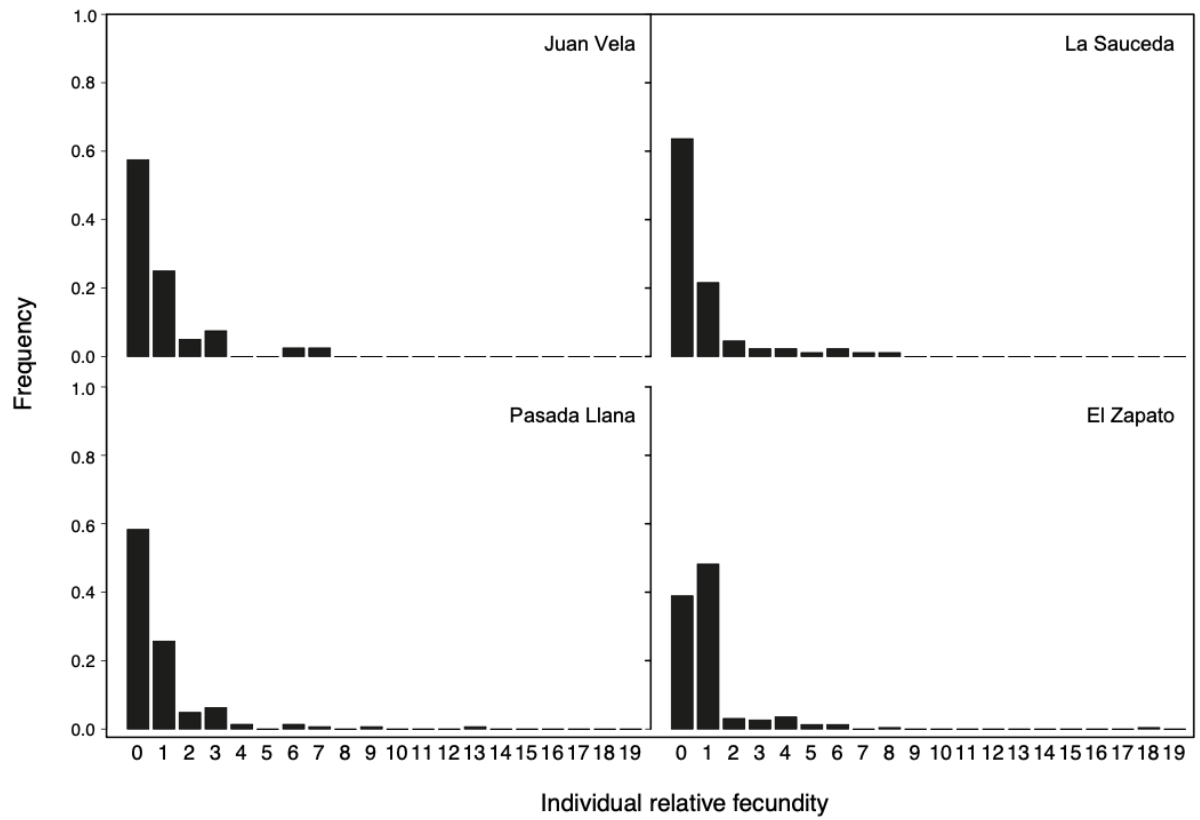


Figure S5. Population-wide mating networks based on inference from the pollen dispersal kernels derived with MEMM. Circles represent individual trees and links denote the estimated probability of mating events among the mapped individuals of each population. Each line represents a probability higher than 0.05 of siring events that a given mother is inferred to have from a given father, with thickness proportional to this probability. This threshold was chosen for illustrative purposes, as mating events are extremely unlikely below it. Areas concentrating likely mating events (thicker links among trees in the map) are distinctly localized among closely-growing trees. Right panels: the corresponding weighted adjacency matrices for the mating graphs of each population. Each square is a combination of pollen donor (rows) and mother tree (column), with color darkness proportional to the probability of mating. Segments to the left indicate scale (bar= 100 m).

